Carbon 136 (2018) 211–216

Contents lists available at ScienceDirect

Carbon

journal homepage: www.elsevier.com/locate/carbon

Large, non-saturating magnetoresistance in single layer chemical vapor deposition graphene with an h-BN capping layer

Chiashain Chuang [a, b], C.-T. Liang [c, *], Gil-Ho Kim [d], R.E. Elmquist [e], Y. Yang [e], Y.P. Hsieh [b], Dinesh K. Patel [c], K. Watanabe [f], T. Taniguchi [f], N. Aoki [a, **]

[a] Graduate School of Engineering, Chiba University, Chiba 263-8522, Japan
[b] Institute of Atomic and Molecular Sciences, Academia Sinica, Taipei 10617, Taiwan
[c] Department of Physics, National Taiwan University, Taipei 10617, Taiwan
[d] School of Electronic and Electrical Engineering, Sungkyunkwan University, Suwon 16419, Republic of Korea
[e] National Institute of Standard and Technology (NIST), Gaithersburg MD 20899, USA
[f] Advanced Materials Laboratory, National Institute for Materials Science, 1-1 Namki, Tsukuba, 305-0044, Japan

A R T I C L E I N F O

Article history:
Received 6 February 2018
Received in revised form
16 April 2018
Accepted 23 April 2018
Available online 26 April 2018

A B S T R A C T

We report large, non-saturating magnetoresistance (MR) of ~140% in single layer chemical vapor deposition (CVD) graphene with an h-BN capping layer at room temperature at $B = 9\,T$. Based on the classical model developed by Parish and Littlewood, our results show that the MR is proportional to the average mobility $< \mu >$ and decreases with increasing temperature. In contrast, in a large-area, extremely homogenous single layer epitaxial graphene (EG) device, the MR is saturating and is inversely proportional to $<\mu>$, which is consistent with the finite resistance network picture. By comparing the results obtained from CVD graphene with an h-BN capping layer with those from the EG device, we show that the non-saturating linear characteristics come from multi-channel current paths in a two-dimensional plane due to the intrinsic grain boundaries and domains of CVD graphene by capping an h-BN layer that increase the $<\mu>$ of CVD graphene. Our results on CVD graphene with an h-BN capping layer pave the way for industrial schemes of graphene-based and air-stable magnetic field sensors with a linear, large response at room temperature.

1. Introduction

Linear magnetoresistance (LMR) is an interesting effect in condensed matter physics because of its possible day-to-day applications in information storages, magnetic sensor readers and magnetic field calibrations [1]. The explanation of the LMR based on theoretical quantum model proposed by Abrikosov is not suitable for the observed magnetoresistance (MR) at room temperature (RT) since no quantum effects are anticipated at RT [2]. Instead, the temperature-dependent LMR in doped silver chalcogenides can be interpreted well by the classical model proposed by Parish and Littlewood (PL) [3–6]. Based on the PL model, the macroscopically disordered and strongly inhomogeneous semiconductor that reveal non-saturating MR at RT can be treated as the coupling among individual inhomogeneous semiconductor regions as random resistor networks [3]. Normally, the MR value in the PL model reveals a quadratic dependence in the low field regime, linear dependence in the intermediate field regime, and saturated behaviour in the high field regime.

$$MR = \frac{\Delta R}{R} \propto \begin{cases} (\mu B)^2, & when\ \mu B < 1; \\ C, & when\ \mu B > 1, \end{cases} \tag{1}$$

where $MR = [(R(B) - R(0))/R(0)]$, $R(B)$ and $R(0)$ are the resistivity at a magnetic field B and at zero magnetic field [3,10], and μ is carrier mobility. In the high field regime, MR $\propto <\mu>$ for $\Delta\,\mu/<\mu> < 1$ and MR $\propto \Delta\,\mu$ for $\Delta\,\mu/<\mu>> 1$, where $<\mu>$ is the average mobility and $\Delta\,\mu$ is the disorder width of the mobility in PL model [3]. Such a classical PL model even can efficiently interpret the two-dimensional (2D) systems, like gold nanoparticle arrayed graphene [7] and bilayer mosaic graphene due to the 2D resistor network [8].

* Corresponding author.
** Corresponding author.
E-mail addresses: ctliang@phys.ntu.edu.tw (C.-T. Liang), n-aoki@faculty.chiba-u.jp (N. Aoki).

https://doi.org/10.1016/j.carbon.2018.04.067

Recently, the effect of top and bottom capping of exfoliated few-layer graphene with hexagonal boron nitride (h-BN) has been shown to increase the carrier mobility of the surface layers, but also to increase the MR value by more than 1000% at RT [9]. Such interesting results could generally be related to the classical PL model due to the weak coupling between 2D graphene layer channels. Moreover, the thickness-dependent exfoliated graphene and graphene foam LMR values at RT are also consistent with the classical PL model and multi-channel model due to graphene multilayer and foam couplings with different carrier mobility and carrier density regarded as three dimensional resistor networks [10,11].

In order to find possible magnetic sensing and storage schemes in graphene-based industry scheme, one may use single-layer chemical vapor deposition (CVD) graphene due to its cost-effectiveness, large-area, ultra-thin scale and effective productions [12]. However, the moderate carrier mobility single-layer CVD graphene may not show well-defined LMR at RT [13] due to its intrinsic grain boundaries, merged domains, impurities and defects although these disordered properties on single-layer CVD graphene are good characterizations, which showed nice LMR at the layer-by-layer vertically CVD graphene with conducting Au and Co junction device [14], for classical PL resistor network model. To the best of our knowledge, LMR in single-layer CVD graphene system has not been observed, which is an urgent issue to be improved for the thinnest scale of graphene-based industrial-like applications.

Here we report large LMR up to ~140% in single-layer CVD graphene with an h-BN capping layer (at $B = 9$ T) at RT. Our results show that the MR is proportional to the average mobility $<\mu>$ and decreases with increasing temperature, which support the classical PL model. In a millimeter-scale homogeneous single-layer EG device [15,16], the MR is saturating in the high field regime and is inversely proportional to $<\mu>$, which agrees with the finite resistor network picture [3]. Furthermore, detailed disordered-related LMR in a single layer graphene system was carried out. Consequently, we suggest that the non-saturating linear characteristics come from multi-channel current paths in a 2D plane due to the intrinsic grain boundaries and domains of CVD graphene by capping an h-BN layer that increases the $<\mu>$ of CVD graphene. Our results on CVD graphene pave the way for industrial schemes of graphene-based and air-stable magnetic field sensors with a linear, large response at RT.

2. Experimental

We used the scotch tape method to mechanically exfoliate homogenous and high quality h-BN flakes [17] and dry-transferred them drily by Gel-Pak polymer [18] onto a commercial single layer CVD graphene/SiO_2/Si substrate [19]. The outward h-BN/CVD graphene region was etched by oxygen plasma, so we can confine the CVD graphene region under the h-BN capping sheet. CF_4 gas was used to etch h-BN capping layer protected by photo-resist for Cr/Au metal depositions as shown in Fig. 1 (a) bottom inset. Firstly, single-layer graphene sample was grown on a chemical-mechanical planarization-polished 4H-SiC (0001) wafer at 1900 °C for 446 s under 98 kPa Ar gas pressure by using a controlled Si sublimation process [15,16,20–22]. Secondly, we directly deposited a metal bilayer (5 nm + 10 nm Au) on single-layer EG so as to avoid pollution from photo-resist residues and produce low-carrier-density EG Ref. [20]. In order to prepare extreme homogeneous of single-layer EG film, we fabricated millimeter-scale EG Hall devices by standard optical lithography processes and removed the protective metal from the Hall bars using diluted aqua regia [20]. Such the extreme homogeneity of single-layer EG film can be characterized by optical microscopy, Raman spectroscopy and atomic force microscopy [15]. (see Supporting Information) Four-terminal longitudinal ρ_{xx} and transverse R_{xy} were measured by standard ac lock-in methods.

3. Results and discussions

As shown in Fig. 1 (a), the MR values of the CVD graphene with an h-BN capping layer device for $T = 50$ K–295 K. In the low field regime, MR values showed a quadratic B dependence and a linear property at high field regime near RT range, which were typical characterizations for LMR [3,21]. Based on the PL classical model, the crossover magnetic field B_C is in between quadratic and linear dependence regime [3], which can be determined from the dotted line and red solid line trace by taking the first-order derivative of MR with respect to B for $T = 295$ K as shown in the inset of Fig. 1(a). According to our analysis and results, the B_C is smaller than $B = 0.9$ T at all temperature range. As shown in Fig. 1(b), the slope of the well-defined linear fit in the MR values versus B^2 within 0.2–0.7 T^2 for $T = 120$ K–295 K, which can determine the average mobility $<\mu>$ due to classical transport behaviors for MR $\propto (\mu B)^2$ [10,23]. Furthermore, the corresponding Hall resistivity $\rho_{xy}(B)$ show nonlinear behaviors in the high field regime at various temperatures, which suggest carrier conductions from different current channels in a 2D plane as shown in inset of Fig. 1(b) which is similar to the multi-layer graphene systems [9]. Consistently, our results agree with the graphene thickness-dependent magnetotransport behaviors for multi-channel model, but in a single-layer CVD graphene with an h-BN capping layer [9,10].

We are able to calculate $<\mu>$ in the range 0.2 $T^2 \leq B^2 \leq$ 0.7 T^2 in our device as shown in Fig. 1 (b). Fig. 2 (a) shows that the $<\mu>$ values decreased from ~2800 to ~2670 $cm^2V^{-1}s^{-1}$ as the temperature is increased from 120 K to 295 K. Also, the MR value decreased with increasing temperature as shown in Fig. 2 (b). Consequently, the MR is nearly proportional to $<\mu>$ in our device as shown in Fig. 2 (c), which highly agrees with the classical PL model [3,10]. On the other hand, we also calculated the Hall mobility μ_H and carrier density n_H so as to compare with $<\mu>$ when increasing temperature as shown in Fig. 2 (d) and inset. Interestingly, the μ_H, and $<\mu>$ slightly decreased when increasing temperature, which indicated the weak electron-phonon coupling from SiO_2 substrate due to the highly disordered CVD graphene property and excellent heat and carrier transferring h-BN capping layer [24–26].

In order to further confirm our speculations, the LMR at RT in single-layer CVD graphene with an h-BN layer is due to the multi-channel model in a 2D plane when current passed through grain boundaries so as to be divided into many current paths as random resistor networks based on the classical PL model [3]. Therefore, we particularly fabricate extremely homogeneous single-layer graphene film with large-area by epitaxial growth method [15] (see supporting information for the optical microscopy, Raman spectroscopy and atomic force microscopy characterizations). As shown in Fig. 3 (a), the longitudinal resistivity ρ_{xx} and Hall resistivity ρ_{xy} with $B = 9$ T at $T = 1.5$ K. The ρ_{xx} approaches zero for $B > 2$ T and the ρ_{xy} laid precisely in wide plateau with filling factor $\nu = 2$, which are typical characterizations for quantum Hall EG device with $\mu_H = 7200$ $cm^2V^{-1}s^{-1}$ and $n_H = 4.2 \times 10^{10}$ cm^{-2} for less disordered property and high quality of our large-area single layer EG device [15,20]. As shown in Fig. 3 (b), the ρ_{xx} gradually increases up in the high field regime while increasing temperature from $T = 1.5$ K–300 K and revealed LMR with saturated behavior near high field regime due to the extremely homogenous monolayer EG film regarded as finite resistance network from the classical PL model as our previous studies [3,21].

The saturated MR values at $B = 9$ T increased while increasing temperature from $T = 200$–300 K in this large-area homogeneous EG device. Again, MR showed a quadratic B dependence at low field

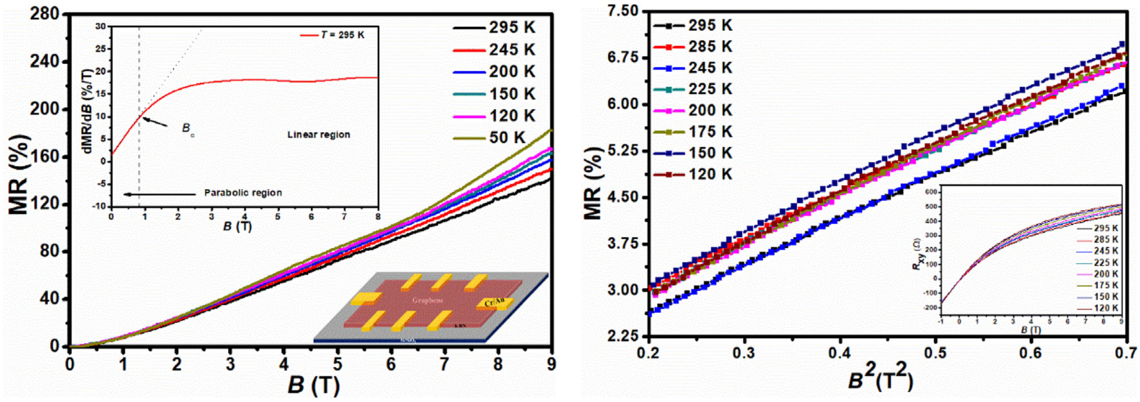

Fig. 1. (a) The MR verses magnetic field B from $T = 50$ K–295 K. The top inset is the differential MR with B, and the B_C is marked the end of linear fitting line and solid line. The bottom inset is the schematic diagram of CVD graphene with h-BN capping layer device. (b) The linear increment in MR with B^2 shows the quadratic dependence from 0.2 to 0.7 T^2. The figure inset is R_{xy} versus B from 120 K to 295 K. (A colour version of this figure can be viewed online.)

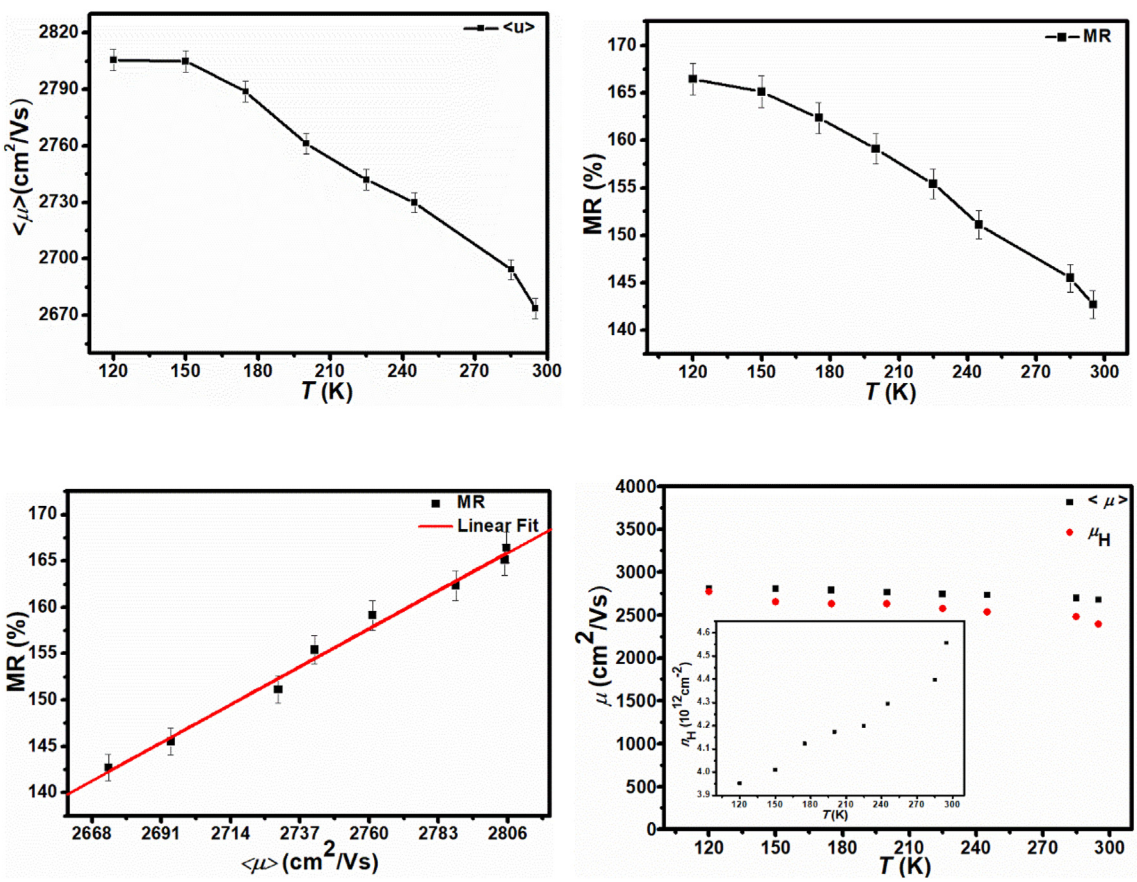

Fig. 2. (a) T dependence of the $<\mu>$ inferred from the fitted slope in Fig. 1 (b). (b) Temperature dependent MR values at $B = 9$ T from the MR versus B curve in Fig. 1 (a). (c) At $B = 9$ T, the MR as function of $<\mu>$. The red line represents a linear fit. (d) Comparison of $<\mu>$ and μ_H with T. The figure inset shows n_H versus T. (A colour version of this figure can be viewed online.)

regime, that we can determine B_C as shown in the inset of Fig. 4 (a) for $T = 300$ K, and saturated at high field regime, which were usual LMR characterizations for our homogenous EG device [3,21]. Hence, we were able to calculate $<\mu>$ in the linear field range $0.2\ T^2 \le B^2 \le 0.6\ T^2$ in our large-area EG device as shown in Fig. 4 (b), and the Hall resistivity ρ_{xy} also revealed nonlinear behaviors on high field regimes at various temperatures due to the contributions from finite carrier channel conductions in a 2D plane as shown in inset of Fig. 4 (b) [9,10], which is further supportive of our speculations for finite conduction channels in a less disordered 2D plane [3,10]. In comparison to CVD graphene without h-BN capping layer, the MR value could not reveal clear LMR behavior [13] possibly due to finite carrier mobility, which is not similar to our clean large-area EG system. On the other hand, a possible reason for observing the large and non-saturated LMR value in the h-BN capped CVD graphene is that the large enhancement of CVD graphene average mobility for MR $\propto <\mu>$ for $\Delta\mu/<\mu> < 1$ [3] which is due to a capping h-BN layer for a flatter CVD graphene surface so as to highly increase the

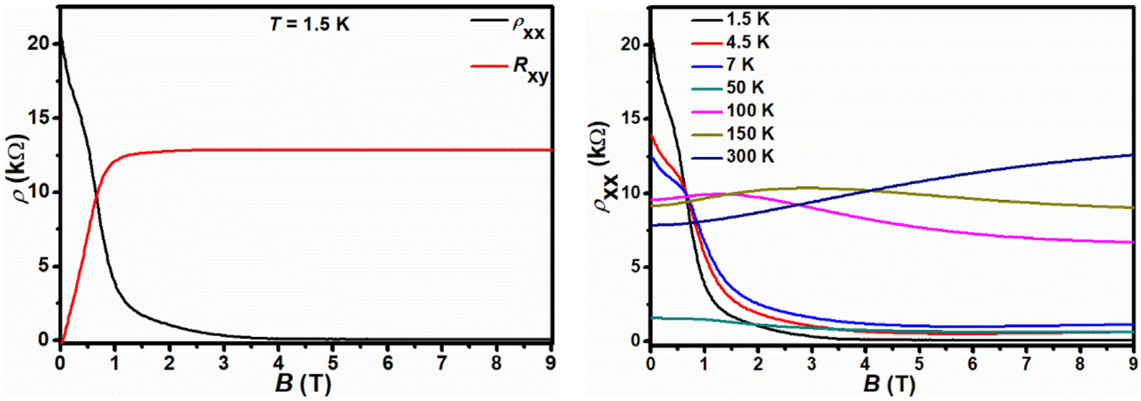

Fig. 3. (a) The ρ_{xx} (black line) and ρ_{xy} (red line) versus B at $T = 1.5$ K in single-layer large-area homogenous epitaxial graphene. (b) The ρ_{xx} versus B at various temperatures. (A colour version of this figure can be viewed online.)

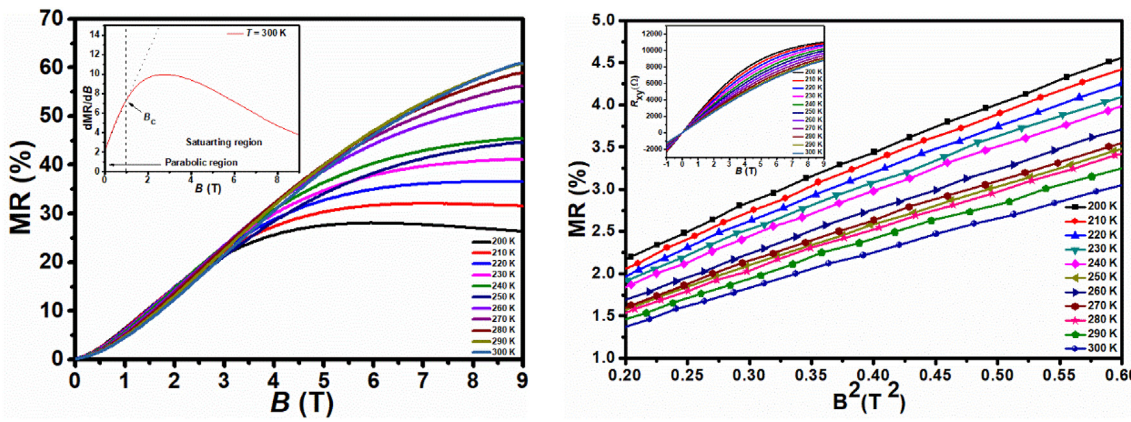

Fig. 4. (a) MR as a function of B at different temperatures from 200 K to 300 K in single-layer large-area homogenous epitaxial graphene. The figure inset shows the saturating behavior of differential MR with B at 300 K near high field regime. (b) It shows linear behavior of MR with B^2 at various temperatures from 0.2 to 0.6 T^2. The figure inset shows R_{xy} versus B from 200 K to 300 K. (A colour version of this figure can be viewed online.)

graphene mobility [27]. In our case the h-BN capped graphene still retains intrinsic disordered properties from grain boundaries as lots of random resistance networks which are related to the mechanism for non-saturated MR value in the high field regime [3].

Fig. 5(a) shows that the $<\mu>$ values decreased from ~2440 to ~2050 cm^{2}V^{-1}s^{-1} as temperature increased from 200 K to 300 K and the corresponding saturated MR values at $B = 9$ T increased while increasing temperature as shown in Fig. 5(b) that is different from the disordered single-layer CVD graphene with an h-BN capping layer. Interestingly, the MR is almost inversely proportional to $<\mu>$ in our large-area EG device as shown in Fig. 5(c), which is similar to thin graphene thickness results regarded as finite conduction channels [3,10]. Also, the related changes in μ_H , n_H and $<\mu>$ while increasing temperature as shown in Fig. 5(d) and inset. Obviously, the μ_H, and $<\mu>$ decreased when increasing temperature, which suggests the strongly electron-phonon coupling from SiC substrate and electron-electron interactions at low temperature [22] in comparison with single-layer disordered CVD graphene with a capping h-BN layer and can be supported from $\rho_{xy} - T$ curves in these two devices (see Supporting Information). Therefore, our results consistently prove that disordered properties from grain boundaries from single-layer CVD graphene with a capping h-BN layer could lead many current paths regarded as infinite resistance networks so as to produce non-saturated MR at high field regime in comparison with larger-area homogeneous monolayer EG device regarded as finite resistance networks [3,10,21].

Finally, we comment on that the LMR effect at RT in a single layer graphene system about the disordered properties degree plays an important role for the numbers of resistance networks degree based on classical PL model. Particularly, such one atomic layer scale with highly efficient CVD production method paves the way for the thinnest scale developments in magnetic storage industries and future nanotechnology markets [1]. Consequently, we find that the non-saturating LMR in CVD graphene can be observed by capping an h-BN layer in order to increasing the mobility and could also be controlled to a certain extent through tuning of the sample disordered properties, like grain boundary sizes and positions [28,29] so as to efficiently increase the LMR value at RT for magnetic storage industrial applications.

4. Conclusions

In conclusion, we have reported LMR measurements of single-layer CVD graphene with an h-BN capping layer and large-area homogenous epitaxial graphene, where we proposed that disordered properties regarded as random resistor network. Large non-saturating nearly ~140% LMR at $B = 9$ T was observed in the CVD graphene with an h-BN capping layer at RT. Both of our devices followed with the classical PL model well. Given CVD graphene's promising application in highly efficient production processes and

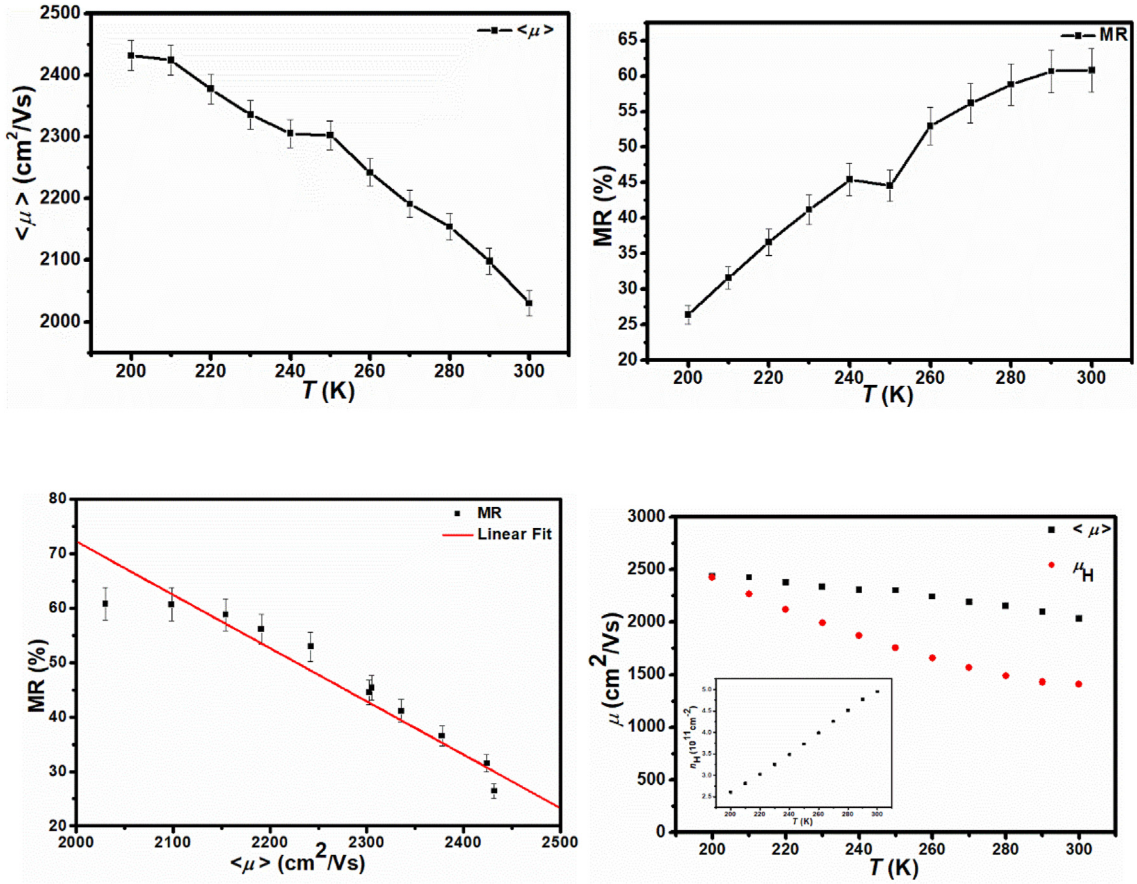

Fig. 5. (a) T dependence of the $<\mu>$ inferred from the fitted slope in Fig. 4 (b). (b) Temperature dependent MR values at $B = 9$ T from the MR versus B curve in Fig. 4 (a). (c) At $B = 9$ T, the MR as function of $<\mu>$. The red line represents a linear fit. (d) Comparison of $<\mu>$ and μ_H with T. The figure inset shows n_H versus T. (A colour version of this figure can be viewed online.)

its scalability, our results point to possible magnetic storage industrial integration of graphene-based magnetic sensors with spintronic devices.

Acknowledgments

As an International Research Fellow of the Japan Society for the Promotion of Science (JSPS), C. Chuang acknowledges a JSPS Postdoctoral Fellowship. C.C. would like to thank Prof. J. P. Bird for useful discussions when he visited Chiba University. C. C. is grateful to the MOST and Institute of Atomic and Molecular Sciences, Academia Sinica for a postdoctoral fellowship under the contract number MOST 106-2811-M-001-164. N.A. acknowledges funding from JSPS KAKENHI (Grant No. JP16H00899 on Innovative Areas "Science of Atomic Layers."

Appendix A. Supplementary data

Supplementary data related to this article can be found at https://doi.org/10.1016/j.carbon.2018.04.067.

References

[1] P. Ripka, M. Janosek, Advances in magnetic field sensors, IEEE Sensor. J. 10 (2010) 1108.

[2] A.A. Abrikosov, Quantum magnetoresistance, Phys. Rev. B 58 (1998) 2788.

[3] M.M. Parish, P.B. Littlewood, Non-saturating magnetoresistance in heavily disordered semiconductors, Nature 426 (2003) 162.

[4] R. Xu, A. Husmann, T.F. Rosenbaum, M.-L. Saboungi, J.E. Enderby, P.B. Littlewood, Large magnetoresistance in non-magnetic silver chalcogenides, Nature 390 (1997) 57.

[5] M. Lee, T.F. Rosenbaum, M.-L. Saboungi, H.S. Schnyders, Band-Gap Tuning, Linear, Magnetoresistance in the silver chalcogenides, Phys. Rev. Lett. 88 (2002) 066602.

[6] A. Husmann, J.B. Betts, G.S. Boebinger, A. Migliori, T.F. Rosenbaum, M.-L. Saboungi, Megagauss sensors, Nature 417 (2002) 421.

[7] Z. Jia, R. Zhang, Q. Han, Q. Yan, R. Zhu, D. Yu, et al., Large tunable linear magnetoresistance in gold nanoparticle decorated graphene, Appl. Phys. Lett. 105 (2014) 143103.

[8] F. Kisslinger, C. Ott, C. Heide, E. Kampert, B. Butz, E. Spiecker, et al., Linear magnetoresistance in mosaic-like bilayer graphene, Nat. Phys. 11 (2015) 650.

[9] K. Gopinadhan, Y.J. Shin, R. Jalil, T. Venkatesan, A.K. Geim, A.H. Castro Neto, et al., Extremely large magnetoresistance in few-layer graphene/boron–nitride heterostructures, Nat. Commun. 6 (2015) 8337.

[10] H. Li, Y.J. Zeng, X.J. Hu, H.H. Zhang, S.C. Ruan, M.J.V. Bael, et al., Thickness-dependent magnetotransport: from multilayer graphene to few-layer graphene, Carbon 124 (2017) 193.

[11] R.U.R. Sagar, M. Galluzzi, C. Wan, K. Shehzad, S.T. Navale, T. Anwar, et al., Large, linear, and tunable positive magnetoresistance of mechanically stable graphene Foam–Toward high-performance magnetic field sensors, ACS Appl. Mater. Interfaces 9 (2017) 1891.

[12] S. Bae, H. Kim, Y. Lee, X. Xu, J.-S. Park, Y. Zheng, et al., Roll-to-roll production of 30-inch graphene films for transparent electrodes, Nat. Nanotechnol. 5 (2010) 574.

[13] A.L. Friedman, J.T. Robinson, F. Keith Perkings, P.M. Cambell, Extraordinary magnetoresistance in shunted chemical vapor deposition grown graphene devices, Appl. Phys. Lett. 99 (2011) 022108.

[14] J.-J. Chen, J. Meng, Y.-B. Zhou, H.-C. Wu, Y.-Q. Bie, Z.-M. Liao, et al., Layer-by-layer assembly of vertically conducting graphene devices, Nat. Commun. 4 (2013) 1921.

[15] Y. Yang, G. Cheng, P. Mende, I.G. Calizo, R.M. Feenstra, C. Chuang, et al., Epitaxial graphene homogeneity and quantum Hall effect in millimeter-scale devices, Carbon 115 (2017) 229.

[16] C. Chuang, Y. Yang, S. Pookpanratana, C.A. Hacker, C.-T. Liang, R.E. Elmquist, Chemical-doping-driven crossover from graphene to "ordinary metal" in

epitaxial graphene grown on SiC, Nanoscale 9 (2017) 11537.
[17] K. Watanabe, T. Taniguchi, H. Kanda, Direct-bandgap properties and evidence for ultraviolet lasing of hexagonal boron nitride single crystal, Nat. Mater. 3 (2004) 404.
[18] A.C. Gomez, M. Buscema, R. Molenaar, V. Singh, L. Janssen, H.S.J.V. Zant, et al., Deterministic transfer of two-dimensional materials by all-dry viscoelastic stamping, 2D Mater. 1 (2014) 011002.
[19] https://graphene-supermarket.com/CVD-Graphene-on-SiO2-Si/(Web page).
[20] Y. Yang, L.-I. Huang, Y. Fukuyama, F.-H. Liu, M.A. Real, P. Barbara, et al., Low Carrier density epitaxial graphene devices on SiC, Small 11 (2015) 90.
[21] C. Chuang, Y. Yang, R.E. Elmquist, C.-T. Liang, Linear magnetoresistance in monolayer epitaxial graphene grown on SiC, Mater. Lett. 174 (2016) 118.
[22] C.-W. Liu, C. Chuang, Y. Yang, R.E. Elmquist, Y.-J. Ho, H.-Y. Lee, C.-T. Liang, Temperature dependence of electron density and electron–electron interactions in monolayer epitaxial graphene grown on SiC, 2D Mater. 4 (2017) 025007.
[23] J.L. Olsen, Electron Transport in Metals, Interscience, New York, 1962.
[24] A.C. Betz, F. Vialla, D. Brunel, C. Voisin, M. Picher, A. Cavanna, et al., Hot electron cooling by acoustic phonons in graphene, Phys. Rev. Lett. 109 (2012) 056805.
[25] Q. Han, T. Gao, R. Zhang, Y. Chen, J. Chen, G. Liu, et al., Highly sensitive hot electron bolometer based on disordered graphene, Sci. Rep. 3 (2013) 3533.
[26] W. Yang, S. Berthou, X. Lu, Q. Wilmart, A. Denis, M. Rosticher, et al., Hyperbolic cooling of a graphene on hBN transistor in the Zener-Klein regime, Nat. Nanotechnol. 13 (2018) 47.
[27] C.R. Dean, A.F. Young, I. Meric, C. Lee, L. Wang, S. Sorgenfrei, K. Watanabe, T. Taniguchi, P. Kim, K.L. Shepard, J. Hone, Nat. Nanotechnol. 5 (2010) 722.
[28] M.V. Kamalakar, C. Groenveld, A. Dankert, S.P. Dash, Long distance spin communication in chemical vapor deposited graphene, Nat. Commun. 6 (2015) 6766.
[29] Y.-F. Lu, S.-T. Lo, J.-C. Lin, W. Zhang, J.-Y. Lu, F.-H. Liu, C.-M. Tseng, Y.-H. Lee, C.-T. Liang, L.-J. Li, ACS Nano 7 (2013) 6522.